Approaching (100)<0vw> by rolling directionally solidified silicon steels

Taeko Yonamine[1] and Fernando JG Landgraf[1]

[1] Instituto de Pesquisas Tecnológicas - IPT, Av. Professor Almeida Prado 532, São Paulo, SP 05508-901, Brazil

Keywords: Silicon steel, Texture, Directional solidification, B_{50}.

Abstract. Based on the possible ability of strip casting to produce (100)<0vw> fiber texture by directional solidification, experiments of rolling, annealing and magnetic measurement were performed on samples that were directionally solidified by other means. Samples with a final texture of strong $(001)<1\bar{2}0>$ component were obtained in steels with 3%Si and 0.2%Al. B_{50} value of 1.71T was obtained in as-cast ring specimen. Starting samples have columnar grain sizes of about 1mm diameter tilted about 9°, on the average, relative to a perfect <100>//ND. Cold rolling produced the expected rotated cube $(001)<1\bar{1}0>$. Further processing steps led to the final texture mentioned above. The paper presents the texture evolution along the processing steps.

Introduction

As mentioned in recent paper [1], the ideal crystallographic texture for use in electrical motors, {100}<0vw>, is found in the section transverse to the columnar growth direction of ferritic steel solidification. The strip casting process produces 2mm thick steel plates directly from the melt and, in general, with favourable conditions for obtaining the ideal texture in the as-cast state. As the 2mm thick plates have to be cold rolled down to 0.5mm for using in motors, the control of the texture during cold rolling is very important since the ideal texture is already present in the as-cast sample.

Experimental

In order to simulate the strip-casting process, directional solidification experiments were performed in a vacuum induction furnace. A 3.0%Si alloy was cast in a 57mm diameter heated ceramic mould (T_{mould} = 1400°C) with a water-cooled copper chill in the bottom. Pouring temperature of 1620°C produced an ingot with columnar grain length of 50mm and with a column diameter of 1mm. For magnetic measurements a ring 1.53mm thick was machined from the ingot and submitted to heat treatment at 760°C for 3h, in a 88%N_2 - 9%H_2 - 3%H_2O atmosphere to decarburise and eliminate residual stresses. Carbon concentration of ring decreased from 260 to 38 ppm. The chemical composition of the sample is given in Table 1.

Table 1. Chemical composition of as-cast annealed ring (wt.%).

%Si	%Al	C (ppm)	S (ppm)	N (ppm)	O (ppm)
3.0	0.2	38	9	16	34

The B_{50} value was determined from magnetization curve at 5mHz. In order to avoid the effect of sample thickness and measuring frequency over the magnet loss, we decided to measure the hysteresis component of total loss obtained from the hysteresis area in the quasi-static condition. As described elsewhere [1] the sample density, 7661 kg/m^3 in this case, was used to calculate hysteresis loss P_H. Another sample was used to study the evolution of texture during two-stage cold rolling. From the same ingot a sheet-shape sample with (39.4x48.4)mm^2 area and 2.6mm thick was machined and submitted to heat treatment at 700°C for 2h, in a 90%N_2 - 10%H_2 atmosphere for stress relief. The sheet sample was submitted to a two-stage cold rolling process. Two techniques were used to determine the texture, microtexture and macrotexture, of silicon steel samples: electron backscattering diffraction (EBSD) and X-ray diffraction, respectively.

Results

Magnetic characterization. The values of B_{50}, dissipated energy W_H and hysteresis loss P_H for as-cast annealed ring are shown in Table 2. It is important to emphasize that hysteresis loss of 1.1 W/kg is the lowest known value obtained in this kind of material. This result could be explained by the good texture (high B_{50}) and low C, N, S, and O concentrations of as-cast sample.

Table 2. B_{50}, dissipated energy W_H and hysteresis loss P_H measured at 1.5T, 60Hz.

B_{50} (T)	W_H (J/m^3)	P_H (W/kg)
1.71	136	1.1

Optical microscopy. The microstructures of sample in each step of experimental procedure are shown in Fig. 1. As we can see in Fig.1a, the effect of cold rolling on the sample microstructure is not uniform and, probably, depends on the grain orientations. Similar behaviour was observed by Hu [2] in his study on silicon-iron single crystals rolled in the (001)[110] and (001)[100] orientations. According to Hu, a (001) crystal rolled along [100] is easy to recrystallize, due to the presence of well-defined deformation bands, whereas a (001) crystal rolled along [110] completely softens without recrystallization. The intermediate annealed sample Fig.1b, is partially recrystallized and presents heterogeneous grain sizes. One can observe recrystallized regions with grain sizes varying from 45μm to 150μm. Comparing Fig.1a to Fig.1b it seems reasonable to conclude that the grains with deformation bands, probably (001)[100] orientation, give rise to the small recrystallized grains after intermediate annealing. The micrograph related to the second cold-rolling was not included in Fig. 1 because there were no visible changes in microstructure. The final annealing (Fig.1c) was not sufficient to perform the complete recrystallization of the sample. The grain size in this stage is almost uniform, around 90μm.

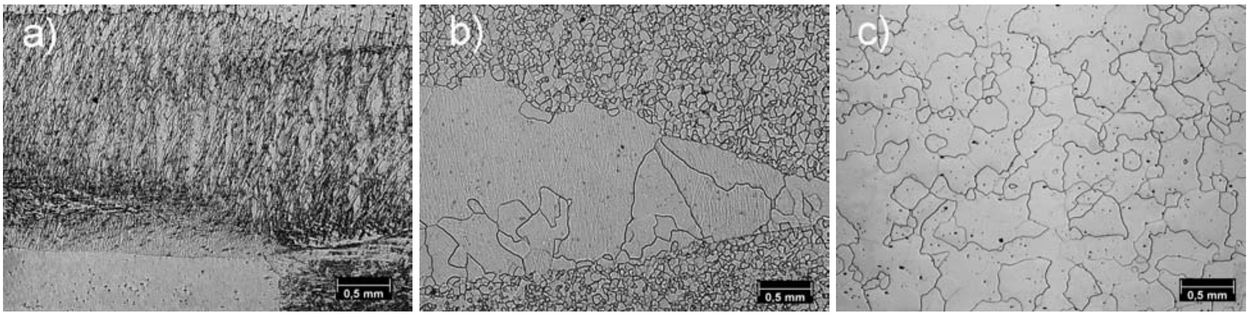

Fig. 1. Optical micrographs of the microstructure after first cold rolling (a), intermediate annealing (b), and final annealing (c)

Texture measurements. The samples in all different steps of two-stage cold rolling process were analysed by X-ray diffraction using Co-Kα radiation. Since the annealed samples presented texture gradient in thickness direction, all texture measurements were performed at the centre of the sample, half thickness from the surface. The orientation distribution functions (ODF) were calculated from three measured incomplete pole figures {110}, {200} and {211} and represented in φ_2 constants sections (φ_2 = 0°, 5°, 10°,…,90°), of the Euler space [3]. In particular, to analyse the φ_2 = 45° section is sufficient, because this section contains at least one of the symmetrically equivalent orientations of the occurring important texture components [4]. The section φ_2 = 45° of ODF for the first cold-rolled sample Fig.2a, presented the maximum intensity of almost 50 times of random distribution at position $(117)<1\bar{1}0>$, near rotated cube $(001)<1\bar{1}0>$. After the intermediate annealing Fig.2b, the maximum intensity of almost 8 times of random distribution was observed at $(114)<\bar{1}\bar{3}1>$, φ_2 = 45° section. In this case, the ODF maximum intensity of almost 13 times of random distribution was observed at position $(392)<17\,\bar{7}\,6>$, φ_2 = 20° section, or, equivalently, at position $(239)<\bar{6}\,\overline{17}\,7>$, φ_2 = 30° section. The decreasing of intensity from 13 to 7 times of random distribution was the main effect of second cold rolling Fig.2c. After final annealing Fig.1d, the maximum intensity of 7 times of random distribution, φ_2 = 45° section, was observed at positions $(001)<1\bar{2}0>$ and $(116)<1\bar{1}0>$ (near rotated cube). These orientations are components of cubic fibre <001> // ND, i.e., components of ideal texture. Therefore, the two-stage cold rolling method resulted in obtaining components of the ideal texture for magnetic properties. Central orientations of cubic fiber, like cube on face $(001)<0\bar{1}0>$, was not observed. Nevertheless, EBSD results that will be presented as follow, show that central orientations are present in the final annealed sample, but due to the texture gradient in thickness direction we couldn't observe them.

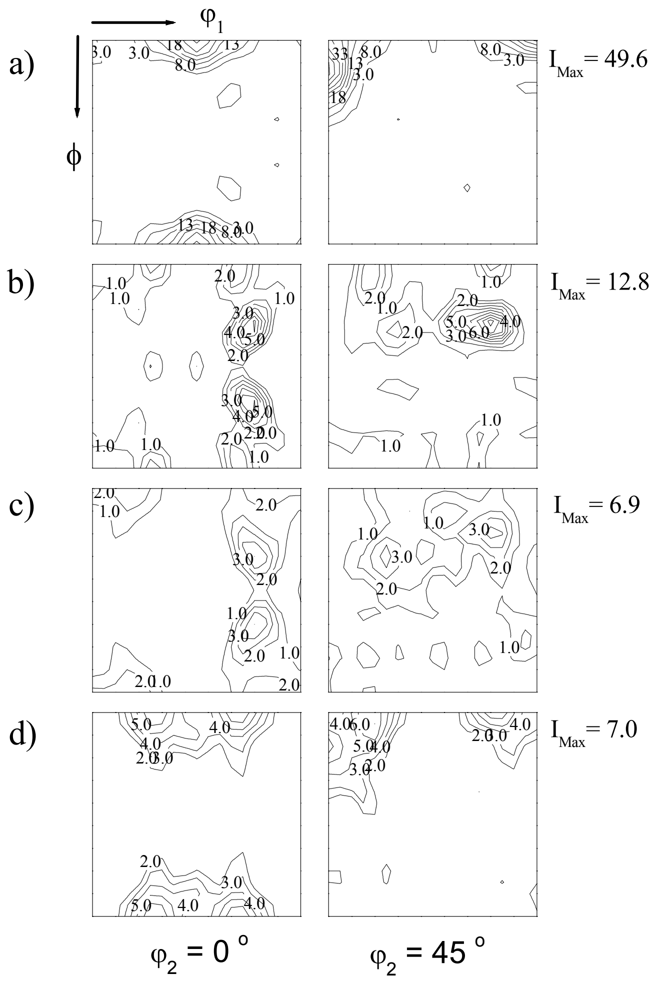

Fig. 2. φ_2 constants sections (φ_2 = 0°, 5°, 10°,…,90°), of the sample after cold rolling (a), intermediate annealing (b), second cold rolling (c), and final annealing (d)

The microtextures of initial, intermediate anneal and final anneal samples were investigated by EBSD. By means of this technique it was possible to determine that grain orientations in as-cast sample were tilted about 9°, on the average, relative to a perfect <100>//ND, i.e., better than the 11° average obtained in recent paper [1]. Five different areas of (1.4x5.2) mm^2 each were used to calculate the average tilt angle. The ODF, φ_2 = 45° section, of intermediate anneal sample, Fig. 3, presented almost the same texture obtained by X-ray diffraction, in which the maximum intensity was observed at $(114)<\bar{1}\bar{3}1>$. Five different areas of (0.34x0.99) mm^2, analyzed by EBSD, presented orientation components of cubic fiber Fig. 4. The Fig.5 corresponds to the average ODF calculated from total area of (1.7x0.99) mm^2, that was not sufficient to reproduce the ODF calculated from X-ray diffraction measurements Fig. 2d. However, this result is useful to show that central orientations of cubic fibre, like cube on face $(001)<0\bar{1}0>$, are present after the final annealing.

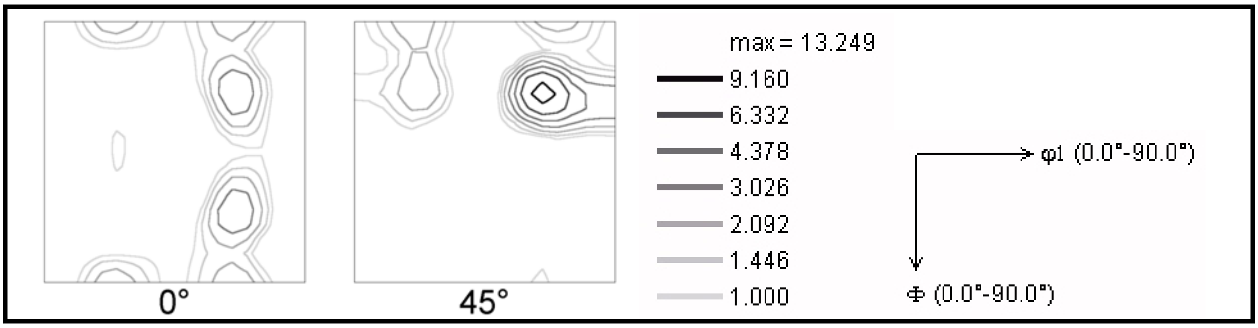

Fig. 3. ODF of intermediate annealed sample measured by EBSD, φ_2 (0^o and 45^o) sections.

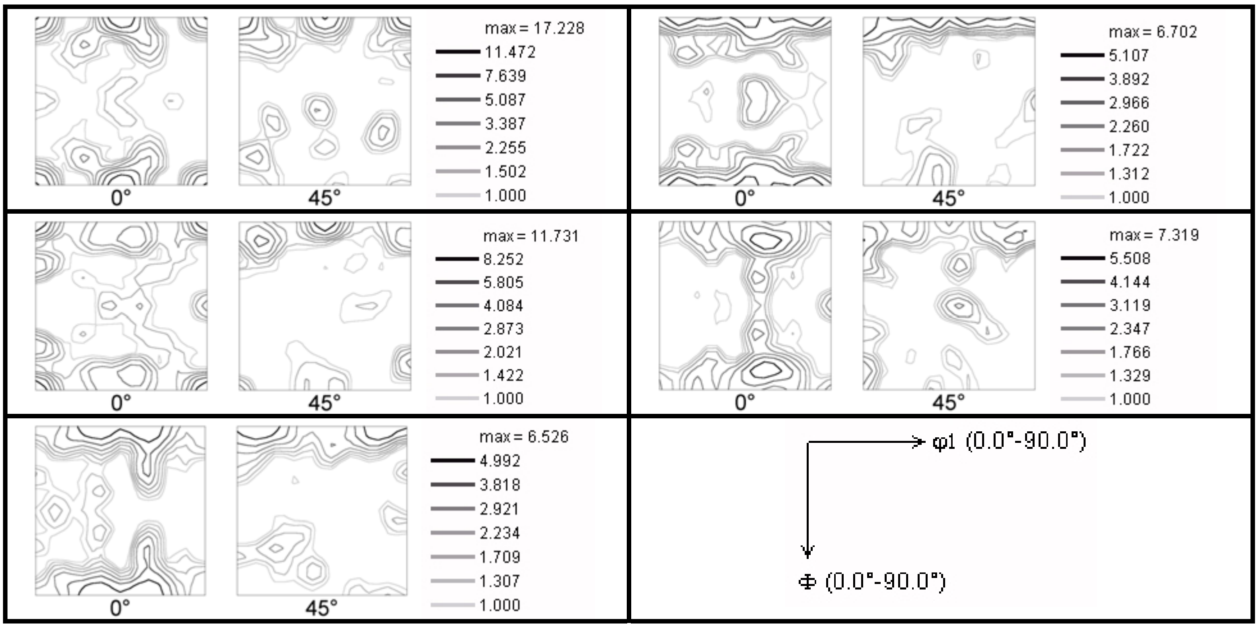

Fig. 4. ODF of final annealed sample measured by EBSD, φ_2 (0^o and 45^o) sections.

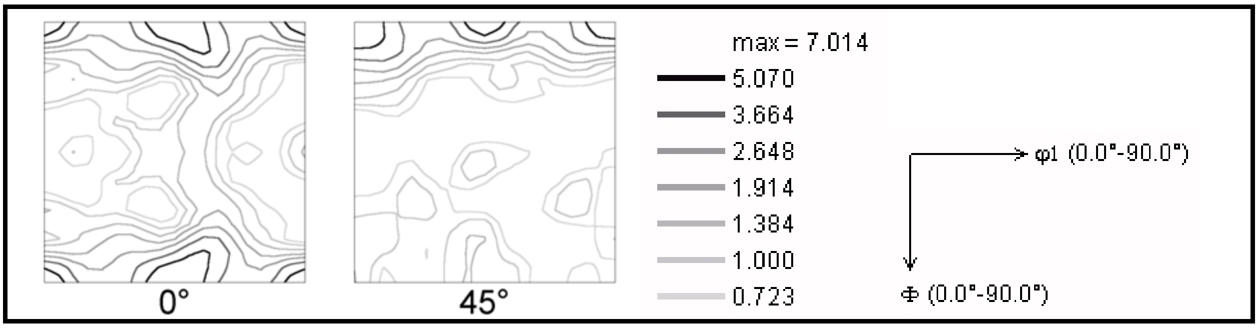

Fig. 5. Average ODF of final annealed sample measured by EBSD, φ_2 (0^o and 45^o) sections.

Conclusions

Heterogeneous deformation structures observed, after first cold rolling, were attributed to the orientation difference between grains. The value of hysteresis loss of 1.1 W/kg, obtained for the as-cast ring, is the lowest known value obtained in this kind of material. By EBSD it was possible to determine that the grain orientations in the as-cast sample are tilted about 9^o from perfect <100>//ND, i.e., better than 11^o obtained in recent paper [1]. The two stage processing developed, after final annealing, high intensities of $(001)<1\bar{2}0>$ and $(116)<1\bar{1}0>$ (near rotated cube). These orientations are components of cubic fibre <001> // ND, i.e., components of ideal texture. It was verified by X-ray texture analysis and confirmed by EBSD.

Acknowledgements: This research was supported by grants from Brazilian agencies FAPESP and CNPq.

References

[1] Landgraf F.J.G., Yonamine T., Takanohashi R., Silva F.Q., Tosetti J.P.V., Beneduce Neto F., Albertin E., Mazzarella V.N.G., Falleiros I.G.S., Emura M., J.Magn.Magn.Mater. **254-255**, (2003), p. 364.

[2] Hsun Hu, Annealing of Silicon-Iron Single Crystals, Recovery and recrystallization of metals, (1963), p. 311.

[3] H.J. Bunge, Texture Analysis in Materials Science, Butterworths, London, (1982).

[4] B. de Boer, J. Wieting, Formation of a near {001}<110> recrystallization texture in electrical steels, Scripta Materialia, **37** (1997) p. 753.